Geol. Mag. **143** (*4*), *2006, pp. 531–543.* © *2006 Cambridge University Press*
doi:10.1017/S0016756805001676 *Printed in the United Kingdom*

Grain-scale deformation in the Palaeoproterozoic Dongargarh Supergroup, central India: implications for shallow crustal deformation mechanisms from microstructural analysis

GAUTAM GHOSH*†, SUKANYA CHAKRABORTY‡,
JOYDIP MUKHOPADHYAY* & ARIJIT RAY*

Department of Geology, Presidency College, 86/1 College Street, Kolkata 700073, India
Geological Studies Unit, Indian Statistical Unit, 203 B.T. Road, Kolkata 700035, India

(*Received* 21 March 2005; *accepted* 21 July 2005)

Abstract – Analysis of the grain-scale deformation mechanisms in folded rocks of the Dongargarh Supergroup, central India, reveals that deformation was accomplished by a combination of pressure solution, microfracturing and dislocation creep processes. The finite strain was assessed using the R_f/ϕ method ($X/Z \approx 2$). Partitioning of strain into various deformation mechanisms revealed that dislocation creep and pressure solution were the major contributors to the finite strain, followed by microfracturing. Analyses of microstructures suggest a sequence of dislocation creep followed by pressure solution and microfracturing, that ultimately gave way to microfracturing and limited crystallization or recrystallization. Overall constancy in volume during deformation is suggested from the balance between fracture-related grain-scale dilatancy and solution-related volume loss. Observations on cleavage spacing within various lithologies in a specific structural setting suggest that lithology played a vital role in cleavage development. Cleavage development in sandstones of the Dongargarh Supergroup required thin shale interbeds (for competency contrast) and grain size < 0.036 mm (4.75 ϕ).

Keywords: cleavage, grain scale deformation, Palaeoproterozoic, shallow crustal processes.

1. Introduction

Microstructures in naturally deformed rocks demonstrate that grain-scale deformation in the upper crust is accommodated by a combination of dislocation creep, diffusion or dissolution creep and microfracturing (Groshong, 1988; Knipe, 1989; Gratier, Renard & Labaume, 1999; Badertscher & Burkhard, 2000; Brodie & Rutter, 2000; Harrison & Onasch, 2000; de Bresser, Evans & Renner, 2002). It is crucial to understand how these processes interact in order to understand the mechanical behaviour of the upper crust and their role in fold-fault and cleavage development.

It has been demonstrated by many workers that position on a fold and proximity to a fault, as well as strain, have predictable effects on cleavage development and cleavage intensity (Alvarez, Engelder & Geiser, 1978; Marshak & Engelder, 1985; Engelder & Marshak, 1985). The role of lithology in cleavage development is less well explored. The importance of clay–quartz matrix within argillaceous limestone and sandstone has been analysed by several workers (Wanless, 1979; Marshak & Engelder, 1985) and the critical amount of matrix to initiate cleavage has been determined as 10 %. However, the roles of layer thickness, grain size, rheology and competence contrast warrant further documentation.

Low-grade greenstone belts with multiple cleavages are suitable candidates for understanding the controlling factors behind sequential cleavage and other microstructural developments. In higher-grade belts the early history of cleavage development is lost due to higher strain and higher metamorphism.

This paper describes attributes of rock cleavage and sequential development of microstructures from a Palaeoproterozoic (Sarkar *et al.* 1967; Sarkar, Gopalan & Trivedi, 1981; Roy, Ramachandra & Bandhyopadhyay, 2000) greenstone belt succession of the Dongargarh Supergroup, central India (Sarkar, 1957–58; Sarkar, Sarkar & Ray, 1994). Detailed microstructural analyses and grain-scale measurements are carried out on two major fold closures and their limbs to understand the role of various deformation mechanisms. Finally, the microstructural analysis attempts to characterize factors, including lithology, that control cleavage development in a low-strain, shallow crustal setting.

2. Geological setting

The Precambrian litho-associations in central India are distributed in two distinct crustal provinces (Ramachandra *et al.* 1998, 2001; Ramachandra & Roy,

† Author for correspondence: gautam_0262@rediffmail.com

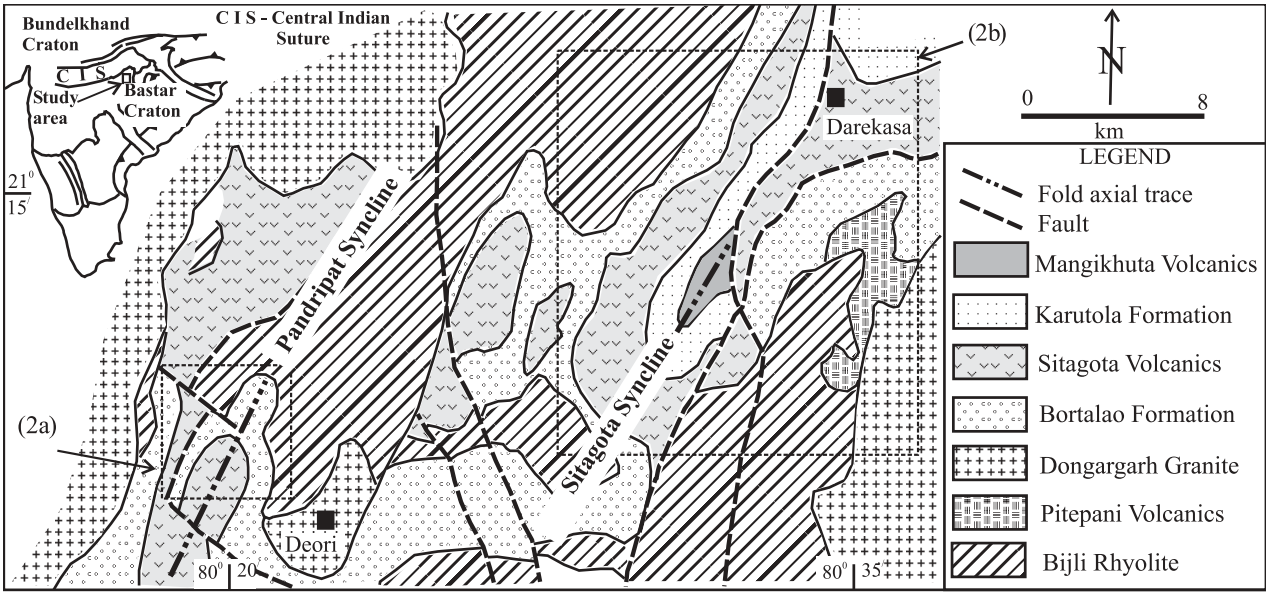

Figure 1. Geological map of the Dongargarh Supergroup, central India, after Sarkar (1957–58); positions of Figure 2a and Figure 2b are shown in two dotted rectangles. Inset shows major tectonic divisions of the Indian shield.

1998), namely the Southern Crustal Province (SCP, Bastar Craton) and the Northern Crustal Province (NCP, Bundelkhand Craton; Fig. 1), which are separated by a crustal-scale shear zone referred to as the Central Indian Suture (Yeddekar *et al.* 1990; Acharyya & Roy, 2000; Bhowmik *et al.* 1999). The Dongargarh Supergroup (Fig. 1) is a predominantly low-grade volcano-sedimentary succession (Deshpande, Mohabey & Deshpande, 1990) in the Bastar Craton (SCP) trending NNE–SSW and extending along strike for about 250 km.

Sarkar (1957–58) and Sarkar, Sarkar & Ray (1994) divided the Dongargarh Supergroup into three groups: Amgaon, Nandgaon and Khairagarh, in ascending order (Table 1). The Amgaon Group is an amphibolite-grade metamorphosed unit with some metasediments, metavolcanics and migmatites. The Nandgaon Group includes a vast suite of volcanic rocks comprising the Bijli Rhyolite (2180 ± 25 Ma: Sarkar, Gopalan & Trivedi, 1981; 2503 ± 35 Ma: Krishnamurthy *et al.* 1990; Mukhopadhyay *et al.* 2001), Pitepani Volcanics and intrusive Dongargarh Granite (2270 ± 90 Ma: Sarkar, Gopalan & Trivedi, 1981; 2465 ± 22 Ma: Krishnamurthy *et al.* 1990). The Khairagarh Group is a sequence of alternating metasediments and volcaniclastics. Both the Nandgaon and Khairagarh groups show greenschist-grade metamorphism (Deshpande, Mohabey & Deshpande, 1990). Yeddekar *et al.* (1990) and Jain, Yeddekar & Nair (1991) suggested that the metavolcanic and metasedimentary associations of the Dongargarh Supergroup represent subduction zone assemblages of the northward-subducting Bastar Craton below the northern Bundelkhand Craton. Alternatively, based on the co-magmatic rhyolite–anorogenic granite assemblage, a continental rift model has been proposed

Table 1 Stratigraphic succession of the Dongargarh Supergroup (after Sarkar, Sarkar & Ray, 1991)

Group	Unit
Chhatisgarh Group	Raipur Group
	Chandarpur Sandstone
	Unconformity
Khairagarh Group	Khairagarh Orogenic phase
	Kotima Volcanics
	Ghogra Formation
	Mangikhuta Volcanics
	Karutola Formation
	Sitagota Volcanics
	Bortalao Formation
	Unconformity
Nandgaon Group	Dongargarh Granite
	Pitepani Volcanics
	Bijli Rhyolite
	Unconformity
Amgaon Group	Amgaon Orogenic phase
	Quartz-sericite schist, feldspathic quartzite, garnet-epidote quartzite, hornblende biotite quartzite, quartz-feldspar biotite gneiss, hornblende schist and amphibolite

for the Dongargarh Supergroup by other workers (Krishnamurthy *et al.* 1990; Gangopadhyay & Ray, 1992, 1997; Neogi, Miura & Hariym, 1996).

The present work involves the lower three units within the Khairagarh Group. The lowermost unit, the Bortalao Formation, comprises basal conglomerate with alternating grit, arkose, siltstone and shale horizons. The Sitagota Volcanics (basalt and andesite) occurring over the Bortalao Formation are succeeded upwards by the Karutola Formation, consisting predominantly of sandstone with minor heteroliths (sand–shale intercalations). Sarkar (1957–58) described 9

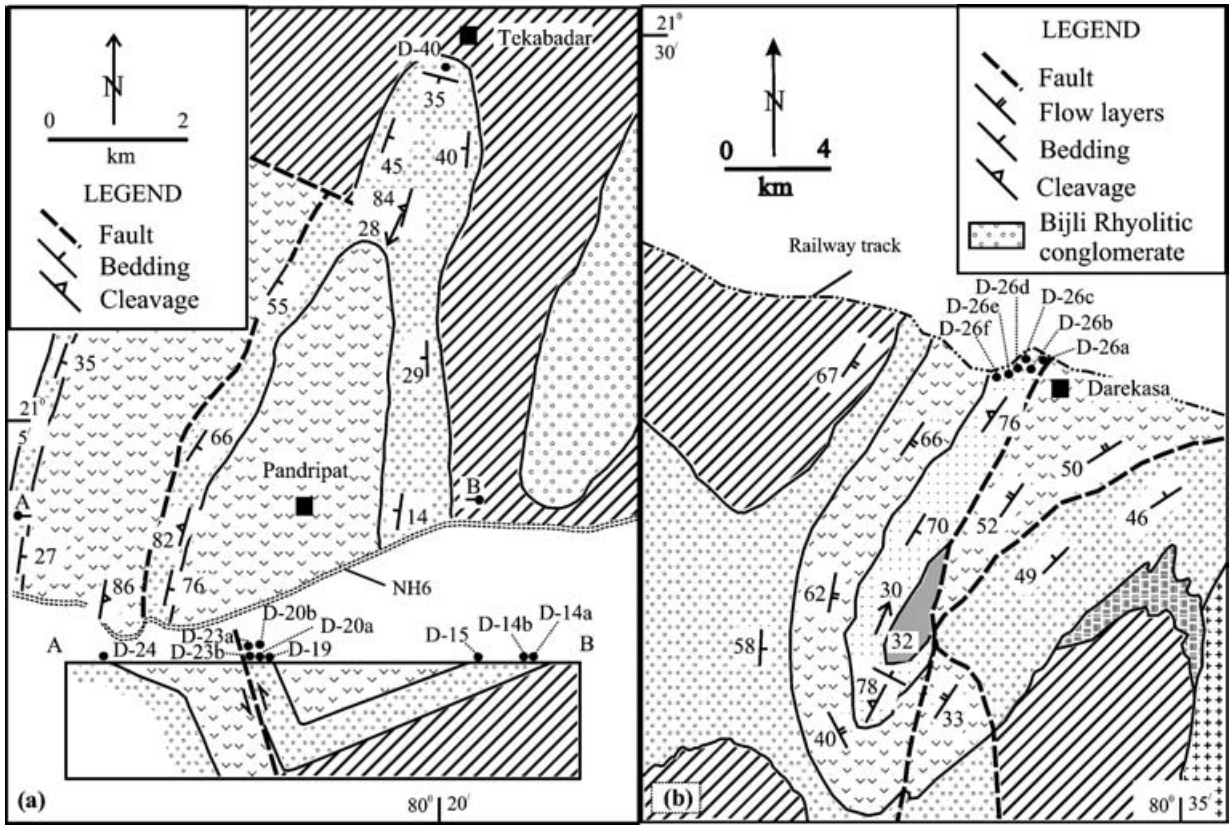

Figure 2. (a) Geological map of the area west of Deori; A–B represents the line of structural section. (b) Geological map of the area west of Darekasa after Gangopadhyay & Ray (1992). D-14 to D-40 represent specimen locations; for other symbols see Figure 1.

major NE–SW-trending folds and about 12 major faults affecting the limbs or the hinges of these regional folds from the rocks of the Khairagarh Group (Fig. 1, Table 1). Most of these faults are N–S trending but some are of E–W trend as well and the different types mainly include normal, reverse and strike-slip faults (Sarkar, 1957–58). Of these, the major focus of our study lies on the Pandripat and Sitagota synclines, located respectively at the western and eastern sides of the outcrop belt of the Khairagarh Group (Fig. 1, Table 1). We present structural and stratigraphic data from the limbs and the hinge of the Pandripat syncline and the western limb of the Sitagota syncline. Thus, both varying lithology and structural positions are observed across the two transects.

3. Cleavage development in relation to major folding

A steep (80° easterly) N–S reverse fault lies at the western limb of the NNE-trending, southerly plunging, asymmetric, Pandripat syncline (Fig. 2a). Two sets of cleavages have been observed across the syncline (Fig. 2a). The first set (S_1) trends N–S, dips steeply towards the west (Fig. 3a) and is axial planar to the major fold. It is well developed at the fold hinge and at the western limb within the fine-grained lithologies (fine-grained arkose, siltstone, shale) of the Bortalao Formation but it is not developed within the gently dipping eastern limb of the fold (Table 2). The second set (S_2: N–S, dips 70–80° easterly; Fig. 3b) is restricted to the vicinity of the fault zone, but is more penetrative than S_1 as far as lithology is concerned, and is present even within coarse-grained rocks of the Bortalao Formation and volcanics of the Sitagota Formation (Table 2). Slickencrysts have developed on bedding at the limbs, particularly within the steeply dipping western limb. The plunge directions of slickencrysts vary systematically across the large fold and have a high-angle relationship with respect to the bedding–cleavage intersection lineation (Fig. 3a). The well-developed cleavage refraction pattern and dominantly axial planar nature of the cleavage (S_1) implies that the folds and cleavage are genetically linked and have resulted from buckling (Ramberg, 1963; Ghosh, 1993, p. 271). However, lack of detectable cleavage fanning suggests their late development in the sequence after sufficient buckle shortening and limb dips have been attained (Mitra & Elliott, 1980; Ford, 1990).

The Sitagota syncline (Fig. 2b) plunges northeasterly at a low angle (Fig. 3c). The axial planar S_1 cleavage (Fig. 3c) is very well developed in the heterolithic unit of the Karutola Formation but is absent from the adjacent Sitagota Volcanics (Table 2). Its geometry varies from a disjunctive slaty cleavage within shale to a spaced, disjunctive cleavage within sandy layers showing excellent cleavage refraction.

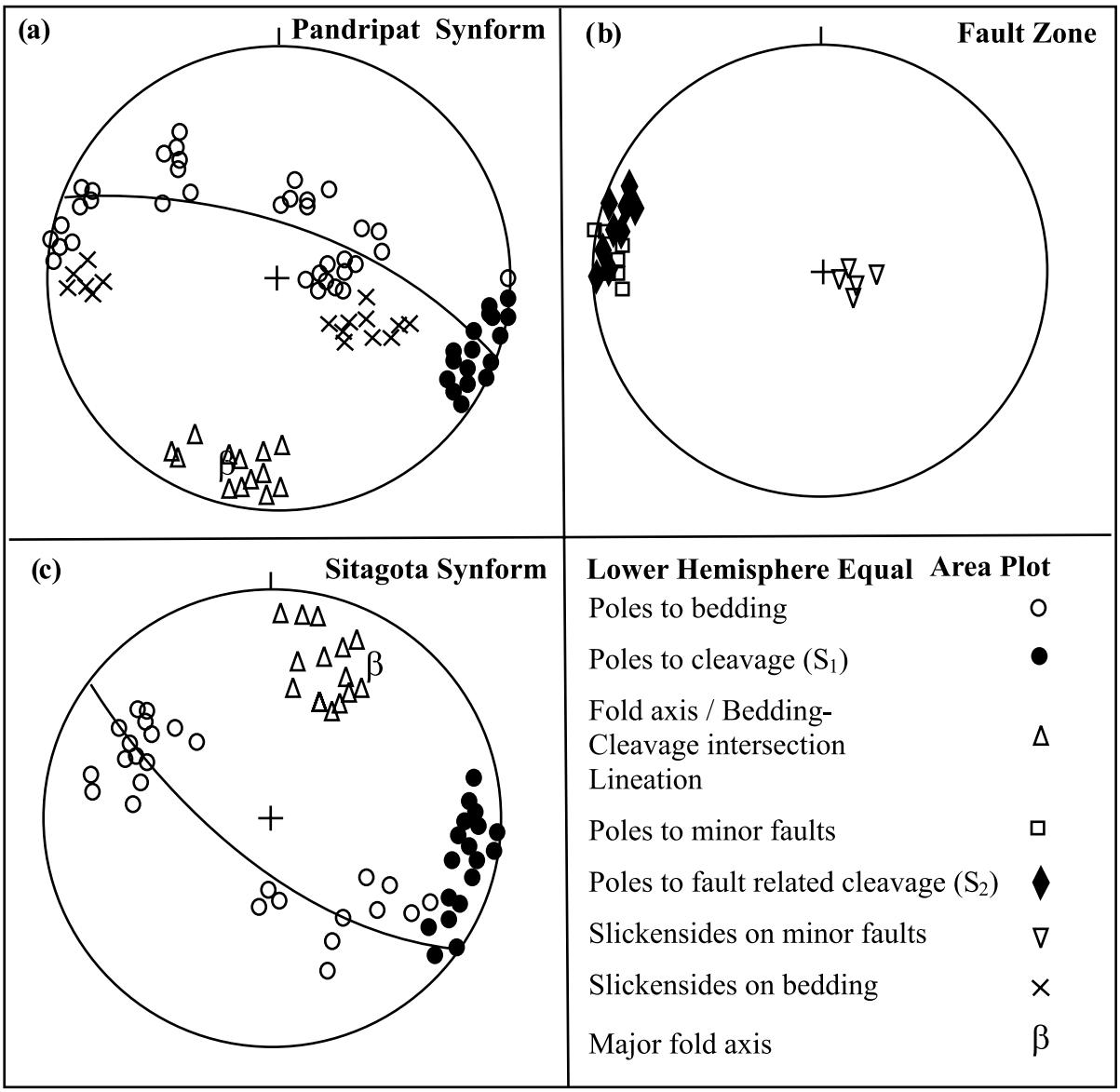

Figure 3. Orientation of different structural elements from the Khairagarh Group. (a) Bedding poles, cleavage poles, fold axes and slickensides on bedding, Pandripat synform; (b) bedding poles, cleavage poles and fold axes, Sitagota synform; (c) cleavage poles, poles to minor faults and slickensides, fault zone–western limb of Sitagota synform; β represents orientation of major fold axis in the area.

Table 2 Distribution of spaced cleavage at different structural settings within the Dongargarh Supergroup

Lithology	Pandripat Syncline				Sitagota Syncline
	Fault Zone	Western Limb	Hinge	Eastern Limb	Western Limb
Bortalao Formation					
Conglomerate and gritty sandstone	P (S_2)	A	–	A	–
Sandstone	P (S_2)	P (S_1)	P (S_1)	A	–
Shale and siltstone	P (S_2)	P (S_1)	P (S_1)	A	–
Sitagota Volcanics	P (S_2)	A	A	A	A
Karutola Formation					
Sandstone	–	–	–	–	P (S_1)
Shale and siltstone	–	–	–	–	P (S_1)

A – Cleavage absent; P – Cleavage present.

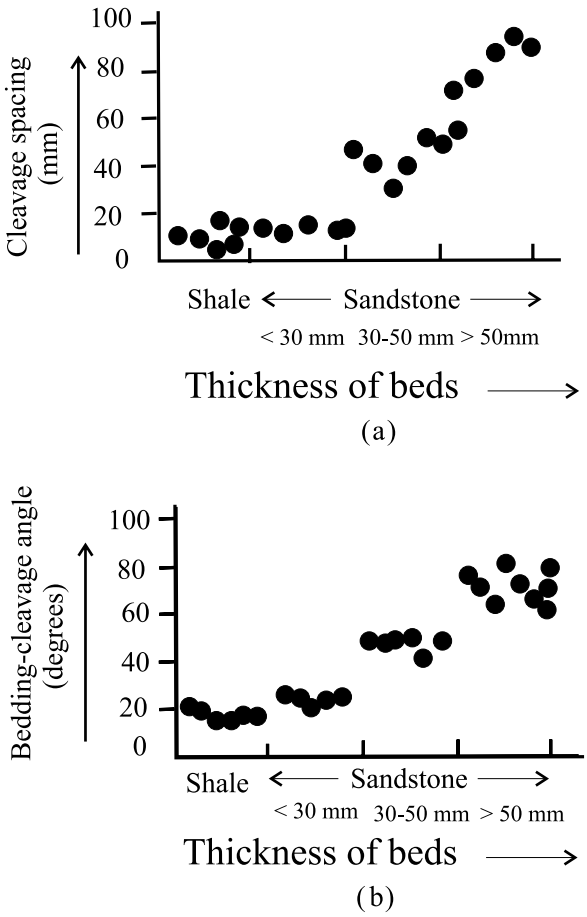

Figure 4. Diagram showing variation in lithology and thickness of beds with (a) cleavage spacing and (b) bedding–cleavage angle.

At the western limb of the Pandripat syncline, thin sandstone beds (thickness < 30 mm) interbedded with shale generally contain better-developed cleavage compared to thick sandstone beds (thickness > 30 mm) with or without shale interbeds. In sandstone beds thicker than 50 mm or grit and conglomerate layers, the cleavage is virtually absent (Fig. 4a). Spacing of disjunctive cleavage domains at mesoscopic scale within shale layers is always less (1 mm to 15 mm) than the sand layers. Cleavage spacing also shows strong dependence on thickness of sand beds and varies from 18 mm to > 60 mm with increasing thickness of beds (Fig. 4a). The cleavage–bedding angle is always low (10–20°) within shale compared to sand-rich layers (30–80°; Fig. 4b). Even within sandstone, cleavage–bedding angle increases with increasing thickness of the sand layers (Figure 4b).

4. Analyses of microstructures

4.a. Cleavage (S_1)

The composition of sandstones varies between sub-quartzarenite to quartzwacke (Table 3). The sandstones from the Karutola Formation are comparatively finer grained, and texturally and compositionally more mature than those from the Bortalao Formation (Table 3). Depending upon the geometry of the cleavage seams and their relation to framework grains, two microstructural varieties of cleavages have been distinguished.

Type-I cleavage has short discontinuous seams around random or crudely oriented framework grains that lack any visible elongation parallel to cleavage (Fig. 5a). Type-II cleavage has well-developed continuous seams developed around framework grains that show elongation parallel to the cleavage (Fig. 5b). The cleavage seams often truncate framework grains (Fig. 5c) and small phyllosilicates recrystallized as beards in pressure shadows of these grains (Fig. 5b).

Intragranular deformation features within framework quartz grains include undulatory extinction, subgrain development, mortar texture, deformation lamellae and deformation bands, indicating the active role of dislocation creep in the shape changes of framework grains (e.g. Poirier, 1985; Tullis & Yund, 1985; Groshong, 1988). In contrast, sutured grain boundaries,

Table 3 Proportion of cleavage, matrix and framework grains within the Dongargarh Supergroup

	Framework grains				
Specimen no.	Quartz (%)	Feldspar (%)	Rock fragments (%)	Recrystallized matrix (%)	Cleavage seam
Bortalao Formation					
D-14a	66.7	11.0	5.7	15.7	0.9
D-15	69.3	3.4	8.7	18.5	0.1
D-19	40.2	0.9	2.4	47.9	8.6
D-20a	38.0	0.0	2.6	55.7	3.7
D-20b	41.7	0.3	1.5	48.4	7.9
D-23a	30.4	2.3	0.4	52.7	14.1
D-23b	37.3	3.1	2.1	42.5	15.0
D-24	44.3	1.4	0.8	47.6	5.8
D-40	39.9	1.7	0.6	42.6	15.2
Karutola Formation					
D-26a	41.9	1.1	0.0	32.0	25
D-26b	49.4	0.5	0.0	33.7	16.3
D-26c	48.5	0.6	0.0	21.3	29.6
D-26d	46.4	0.8	0.0	24.5	28.3
D-26e	44.8	0.0	0.0	27.8	27.2
D-26f	48.4	0.1	0.0	36.2	15.2

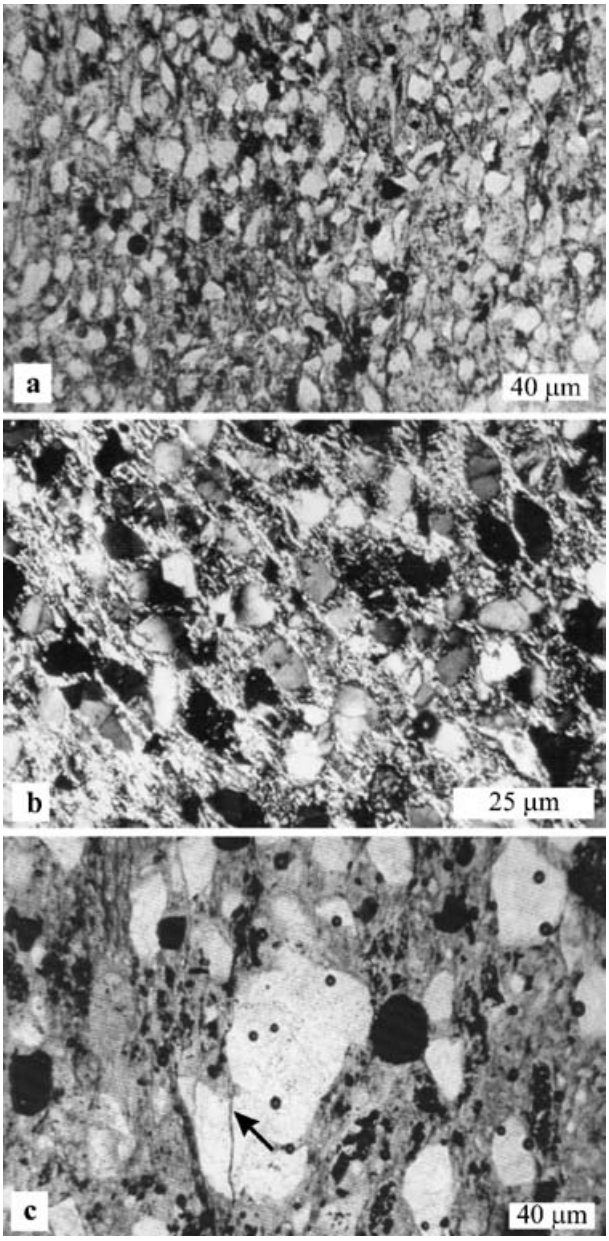

Figure 5. (a) Photomicrograph showing Type-I cleavage fabric, short discontinuous cleavage seams developed along grain boundary of randomly oriented framework grains. (b) Photomicrograph showing Type-II cleavage fabric, continuous cleavage seams around strongly elongated framework grains. (c) Photomicrograph showing anastomosing cleavage seam truncating a large framework grain (see arrow).

truncation of elongated framework grains showing dislocation creep features by cleavage seams (Fig. 5c) and development of mica beards against elongated framework grains (Fig. 5b) suggest that the cleavage fabric is best explained by some form of solution–precipitation process (Williams, 1972; Groshong, 1988; Blenkinshop, 2000) which operated subsequent to accumulation of some amount of crystal plastic strain in framework grains.

Quantification of grain-scale deformation was attempted from specimens of the Bortalao Formation (Wu & Groshong, 1991; see Figs 1, 2a for location). The data indicate (Table 4) that the proportion of grains showing dislocation creep strain is more or less constant (85 to 100 %) from the gently dipping eastern limb to the steeply dipping western limb of the Pandripat syncline. The occurrence of these features is not directly proportional to cleavage development. Rather, uncleaved specimens (such as D-14a–b and D-15) from the eastern limb of the Pandripat syncline also contain abundant dislocation creep features, indicating its early formation (as elongated grains showing crystal plastic slip get truncated by cleavage seams), irrespective of cleavage development in the transect.

Pressure solution matches with dislocation creep at the hinge and steep limb (compare D-40 with D-19–23 in Table 4) of the fold, where late cleavage development is preferentially concentrated. Its proportion is as high as 80–90 % (Table 4) at such sites. However, its near absence from the uncleaved eastern limb is significant in this respect (Table 4). The simultaneous increase in proportion of sutured grain contacts together with development of mica beards against framework grains in cleaved specimens indicate that the rock behaved more or less as a closed system during cleavage formation. Thus pressure solution is preferred over solution transfer in an open system under high fluid pressure (Cox & Etheridge, 1989) where loss of dissolved material would have been more evident.

In general the sandstones from the Bortalao Formation are coarser (> 0.028 mm or $< 5\,\phi$) than psammites from the Karutola Formation (< 0.019 mm or $> 5.5\,\phi$). Sandstones of the Bortalao Formation with grain size > 0.036 mm ($< 4.75\,\phi$) usually lack cleavage, while those with grain size ranging between 0.030 and 0.036 mm (4.75–5 ϕ) show Type-I cleavage fabric (Table 5). Fine-grained (< 0.030 mm or $> 5\,\phi$) rocks of both the Bortalao Formation and Karutola Formation show Type-II cleavage fabric (Table 5). The microstructures of the two varieties of cleavage can be readily explained by increasing dissolution along grain boundaries, with the Type-I cleavage fabric representing an early stage in the development of the solution seams along the boundaries of the framework grains. Further solution along these seams might result in Type-II fabric with well-developed anastomosing seams that link up with seams of adjacent grains to form a continuous network of cleavage.

4.b. Transverse extensional veins

Transverse veins at high angle to cleavage are very common within the rocks. Some of these get folded or displaced by cleavage seams (Fig. 6a) with intra-vein quartz–phyllosilicate showing sparse intra-granular deformation features while some other veins cross-cut cleavage without getting bent or offset and without any

Table 4 Abundances of microstructural features across the Pandripat synform within the Bortalao Formation

			Dislocation creep					Microfracturing					
Specimen no.	Position	Se	We	Sg	Mt	Db	Fl	Tl	If	Tf	Ps	Mica beard	n
D-14a	PSEL	1	99	14	5	0	2	8	31	0	1	0	100
D-14b	PSEL	0	100	23	11	5	5	13	25	0	2	0	100
D-15	PSEL	3	97	26	9	0	0	33	55	29	5	0	100
D-19	PSWL	5	95	19	10	1	9	64	32	4	46	28	100
D-20a	PSWL	15	85	17	9	8	18	51	28	3	54	27	100
D-20b	PSWL	6	94	18	4	9	4	34	18	1	66	12	125
D-24	PSWL	9	90	19	11	3	1	71	13	0	65	8	110
D-23a	FZ	10	91	10	7	4	1	18	23	0	91	83	200
D-23b	FZ	5	95	16	14	3	2	30	14	0	86	76	100
D-40	PSH	7	96	21	12	2	2	26	20	0	90	79	200

Se – Straight extinction; We – Wavy extinction; Sg – Subgrain; Mt – Mortar texture; Db – Deformation band; Fl – Fairbairn lamellae; Tl – Tuttle lamallae; If – Intragranular fracture; Tf – Transgranular fracture; Ps – Pressure solution; PSEL – Eastern limb, Pandripat syncline; PSWL – Western limb, Pandripat syncline; PSH – Hinge, Pandripat syncline; FZ – Fault zone; n – number of grains analysed per thin-section.

Table 5 Variation in cleavage type, proportion of cleavage and grain size of selected samples at different structural sites within the Dongargarh Supergroup

			Cleavage seam			
Specimen no.	Structural position	Mean grain size FG (mm)	Proportion (%)	Length (mm)	Spacing (mm)	Type
Bortalao Formation						
D-19	PSWL	0.033	8.6	0.28	1.92	I
D-20a	PSWL	0.035	3.7	0.21	2.20	I
D-20b	PSWL	0.036	7.9	0.22	2.05	I
D-24	PSWL	0.030	5.8	0.23	2.13	I
D-40	PSH	0.031	15.2	0.77	0.19	II
D-23a	FZ	0.028	14.1	0.75	0.16	II
D-23b	FZ	0.030	15.0	0.83	0.20	II
Karutola Formation						
D-26a	SSWLm	0.006	25.0	1.12	0.04	II
D-26b	SSWLm	0.008	16.3	0.81	0.05	II
D-26c	SSWHm	0.009	29.6	1.65	0.03	II
D-26d	SSWHm	0.019	28.3	1.72	0.04	I
D-26e	SSWLm	0.013	27.2	0.90	0.10	I
D-26f	SSWLm	0.012	15.2	0.64	0.12	II

PSWL – Western limb, Pandripat syncline; PSH – Hinge, Pandripat syncline; FZ – Fault zone; SSWLm – Western limb, Sitagota syncline (from limb of minor fold); SSWHm – Western limb, Sitagota syncline (from hinge of minor fold); FG – framework grains.

evidence of internal deformation in the internal quartz–phyllosilicates. The cross-cutting relations suggest that vein formation (brittle microfracturing) started synchronously with cleavage and continued until the end of the penetrative deformation. The preferential concentration of these veins in the steep western limbs of the synforms and their near absence from the gently dipping eastern limbs suggest that the steep western limbs were suitably oriented with respect to the E–W shortening direction. Consequently the steep western limbs accommodated much of the cleavage parallel extension by developing a set of extension fractures at high angle to cleavage (Fig. 7a).

4.c. Conjugate shear or oblique extension fractures

Trans- to inter-granular fractures (Fig. 6b) are present in single or conjugate sets with cleavage seams getting sharply bent or kinked within these zones (Fig. 6c). This indicates that fracture development post-dates cleavage. However, their preferential occurrence, like the extensional veins, at the hinges and western limbs precludes any major change in the E–W shortening direction during post-cleavage shortening (Fig. 7b). The microfracture sites are usually occupied by spectacular fibrous phyllosilicates and quartz developing a second cleavage (S_{m2}) against which the S_1 gets bent or crenulated (Fig. 6d). The orientation of S_{m2} is similar to the easterly dipping cleavage set (S_2) developed near the reverse fault affecting the western limb of the Pandripat syncline (Fig. 7b). Accordingly, the timing of faulting could be correlated with development of conjugate shear fractures at grain scale.

4.d. Low finite strain regime

Strain measurements (X–Z sections) were carried out from sandstones of the Bortalao Formation and the

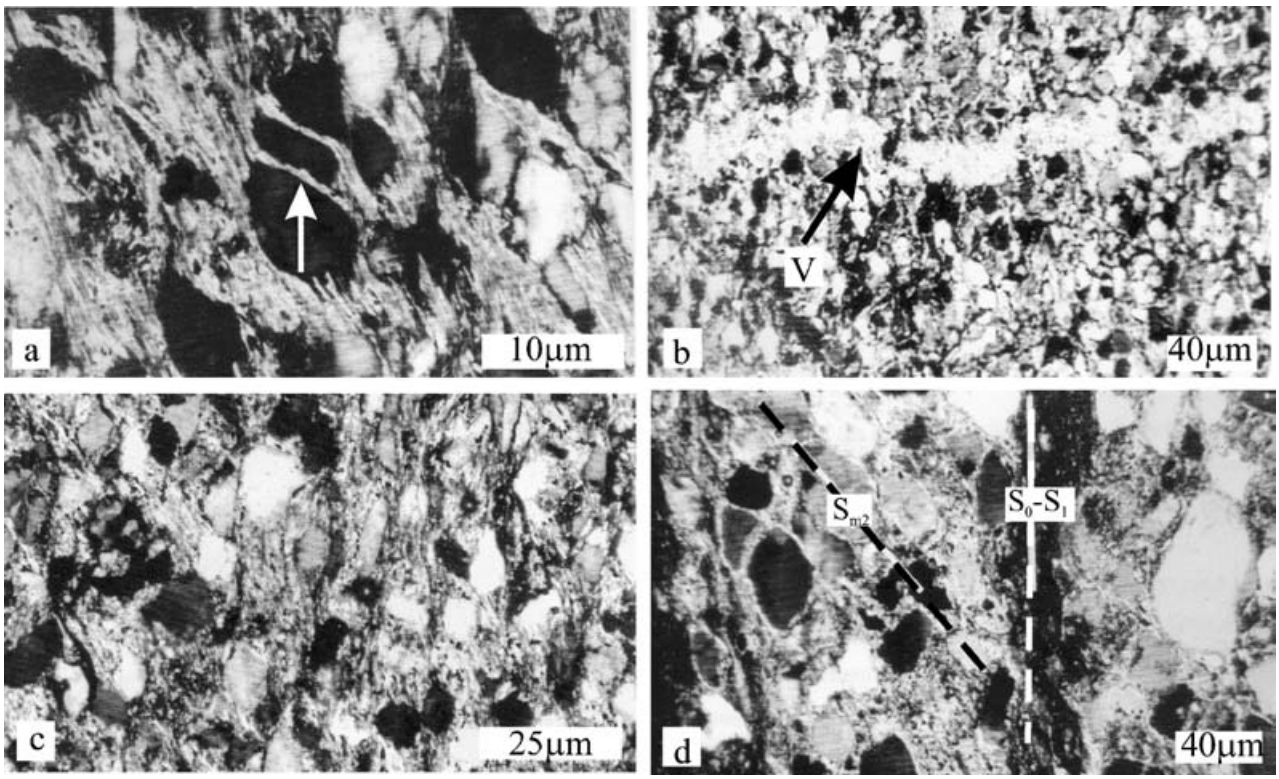

Figure 6. (a) Photomicrograph showing transgranular shear fractures (see white arrow) along which phyllosilicates have recrystallized. (b) Photomicrograph showing a vein (V) developed at high angle to cleavage seams. Note minor warping of the vein and offset along cleavage traces. (c) Photomicrograph showing conjugate transgranular shear fractures. (d) Photomicrograph showing cross-cutting relationship between S_1 cleavage and S_{m2} cleavage. Note bending of S_1 (parallel to S_0) against S_{m2}.

Karutola Formation (see Fig. 2a, b for specimen locations) across the transect. Two-dimensional strain ratios (R_s) are obtained from the data using the hyperbolic net of De Paor (1988) by the R_f/ϕ method (Ramsay, 1967; Dunnet, 1969; Table 6; Fig. 8).

The observed X/Z aspect ratios (1.2–2.1) of strain ellipses limit the amount of shortening to be varying from 10 % to 28 % in the transect. Though data was collected from only two folds within the deformed rocks of the Khairagarh Group, it is worth mentioning here that the folds are spatially separated by at least 20–25 km and occur at the eastern and western extremities of the outcrop of the Khairagarh Group (Fig. 1, Table 1). It can thus be reasonably concluded that the estimated shortening value from the folds is a good first-hand approximation for the Khairagarh Group as a whole.

Measured strain values from different orogenic belts (both collisional and accretionary) across the globe show significantly higher strain values from their internal parts in comparison to the external fold-thrust zones. The Variscans from southwest England show X/Z aspect ratios varying between > 5 and 25 (Rattey & Sanderson, 1982). Strain analysis from the Helvetic nappes of western Switzerland (X/Z aspect ratios 4–20: Ramsay & Huber, 1983; Dietrich, 1989) and the Tasman orogenic belt of southeast Australia (X/Z aspect ratios 3–35: Gray & Willman, 1991) present similar high strain values from internal deformation zones within thrust sheets. The external fold-thrust zones of such orogenic belts show lesser values of

Table 6 R_s–ϕ of selected samples at different structural settings within the Dongargarh Supergroup

Specimen no.	Structural position	R_s	ϕ
Bortalao Formation			
D-19	PSWL	1.7	7°
D-20a	PSWL	1.2	35°
D-20b	PSWL	1.6	22°
D-24	PSWL	1.4	14°
D-40	PSH	2.0	1°
D-23a	FZ	2.1	2°
D-23b	FZ	2.0	3°
Karutola Formation			
D-26a	SSWLm	1.9	−1°
D-26b	SSWLm	1.5	17°
D-26c	SSWHm	2.0	1°
D-26d	SSWHm	2.1	2°
D-26e	SSWLm	1.9	2°
D-26f	SSWLm	1.9	−2°

PSWL – Western limb, Pandripat syncline; PSH – Hinge, Pandripat syncline; FZ – Fault zone; SSWLm – Western limb, Sitagota syncline (from limb of minor fold); SSWHm – Western limb, Sitagota syncline (from hinge of minor fold).

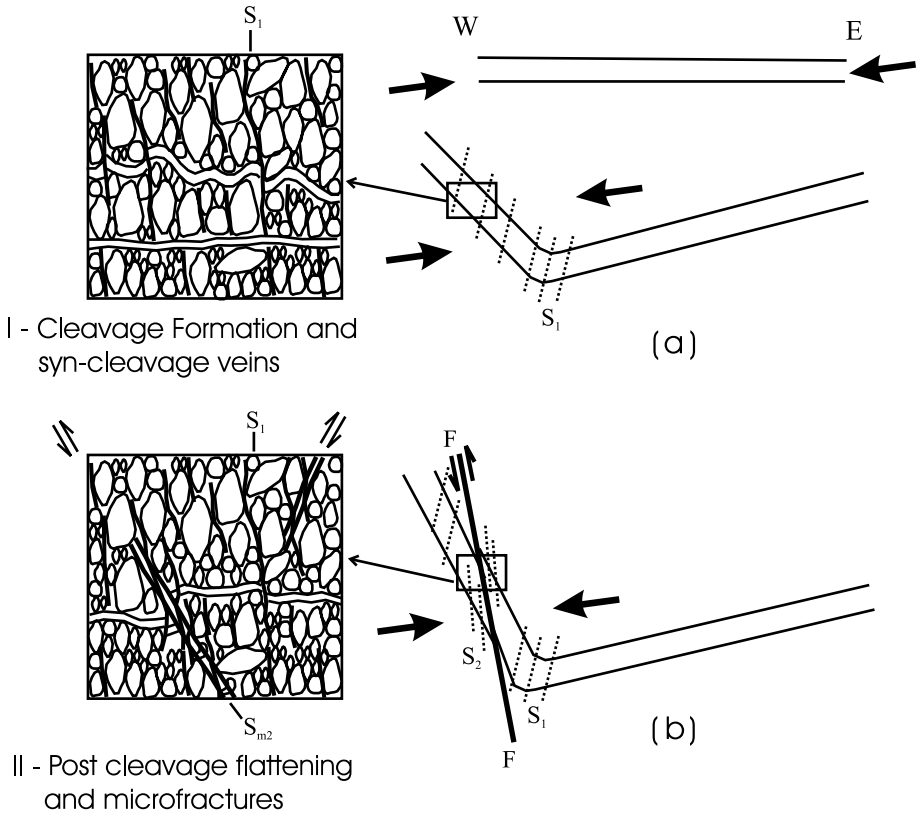

Figure 7. Model showing development of large asymmetric folds within the rocks of the Dongargarh Supergroup with (a) concentration of mesoscopic and microscopic deformation features (cleavage and syn-cleavage veins) at the steep western limb of the fold. (b) Post-cleavage flattening, development of S_2 cleavage and conjugate shear fractures, F–F represents fault plane, dashed lines represent cleavage traces and bold arrows represent direction of shortening.

strain, such as the Southern Adelaide Fold-Thrust belt of south Australia (X/Z aspect ratios 1.2–3: Yassaghi, James & Flottmann, 2000) or the North Mountain thrust sheet, central Appalachians (X/Z aspect ratios 1.07–3.23: Evans & Dunne, 1991). However, the observed strain values (X/Z ≈ 1.2–2.1) from the deformed rocks of the Dongargarh Supergroup in the two transects consistently lie in the lower part of the strain values recorded even from external zones of these orogenic belts.

5. Deformation mechanism association and its implication

Strain related to initial buckling and limb rotation was mostly accommodated through intra-granular crystal plastic processes. Its proportion remains more or less constant at both the limbs of the Pandripat syncline. Pressure solution became the dominant deformation mechanism, producing the visible cleavage fabric during fold tightening, and was preferentially concentrated at the high-strain sites such as the western limb and hinge of the asymmetric fold structure. As a result, concentration of cleavage domains also occurred at such sites, which were more suitably placed than the gently dipping eastern limb with respect to the E–W shortening direction. Pressure solution was accompanied and followed by fracturing and vein formation as microfracturing became important at a later phase. Hence, the specific deformation mechanism sequence for the rocks of the Khairagarh Group turns out to be dislocation creep followed by pressure solution and microfracturing, that ultimately gave way to microfracturing and limited crystallization or recrystallization during progressive growth of the fold, cleavage and fault structures. Deformation by a crystal plastic mechanism (dislocation creep), which dominated initially and controlled early folding, is essentially an isochemical process and thus conserves mass. Pressure solution, which became important during the later stage of fold tightening and cleavage formation, on the other hand, leads to volume loss on the scale of a single grain or several tens of grains, but it was essentially coupled with formation of extensional and shear micro-fractures that lead to grain-scale dilatancy. In effect there was a balance between fracture-related grain-scale dilatancy and solution-related volume loss so that an overall constancy in volume was maintained during deformation of the Khairagarh Group.

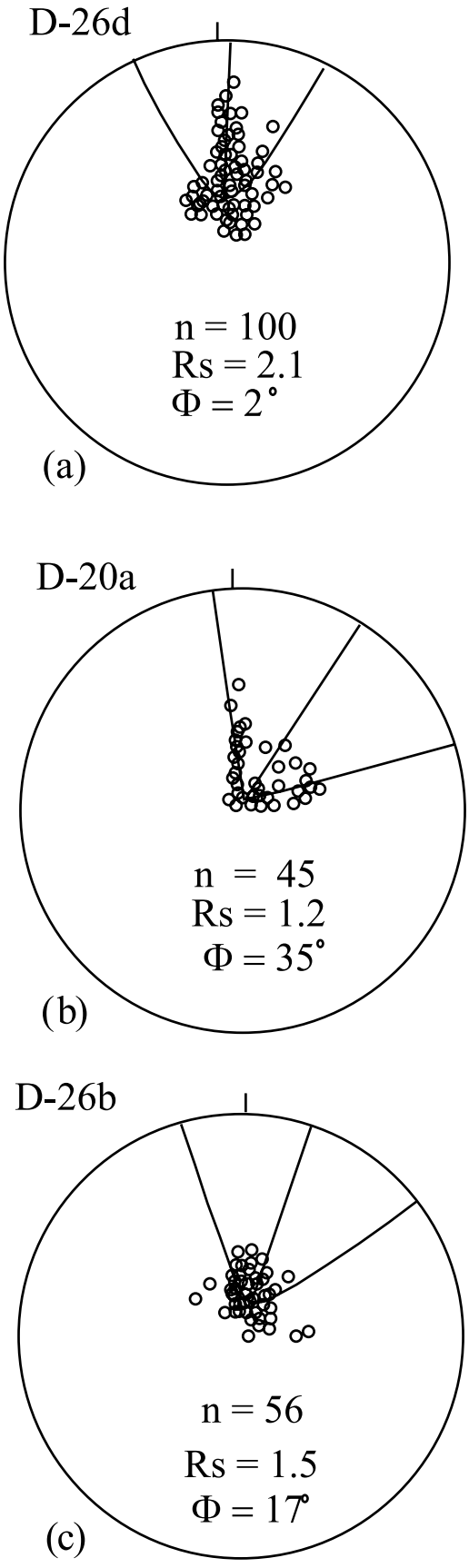

Figure 8. Three representative (a–c) R_f–ϕ plots of deformed sandstones from the Bortalao Formation and Karutola Formation.

Deformation of polymineralic rocks in upper crustal settings often involves more than one deformation mechanism (Groshong, 1988; Knipe, 1989; Badertscher & Burkhard, 2000; Harrison & Onasch, 2000; de Bresser, Evans & Renner, 2002). Formation of cleavage in such a setting essentially involves some form of solution–dissolution processes (Cox & Etheridge, 1989; Roo & Williams, 1990; Blenkinshop, 2000), which are bound to produce volume loss if not counterbalanced by fracture-related dilatancy and recrystallization. Thus a combination of dissolution creep with microfracturing–recrystallization appears to be the real rate-controlling process if volume constancy is to be maintained (Cox & Etheridge, 1989). Addition of dislocation creep to such a deformation mechanism association would not alter the requirement of overall volume constancy at any stage. The present study suggests that this specific sequence of grain-scale processes or the deformation mechanism association of dissolution creep–microfracturing in any combination with dislocation creep could very well be the prevalent grain-scale processes at upper crustal settings if volume constancy during crustal-scale deformation is maintained. A creep law combining such grain-scale deformations would better explain the observable macroscopic processes (fold, fault and cleavage development) at the upper crust, particularly in low grade–low strain belts ($X/Z \approx 2$) without appreciable metamorphic grain growth and grain reorientation.

6. Controls of lithology in cleavage development

Lithology plays a crucial role in development of cleavage morphotypes and cleavage spacing and is believed to control the grain-scale behaviour of materials (Marshak & Engelder, 1985; Engelder & Marshak, 1985). In contrast to pure quartzite or pure sandstone that deform predominantly by intra-crystalline slip, clay-rich impure sandstone and impure limestone develop cleavage by a solution–precipitation process (de Boer, 1977; Marshak & Engelder, 1985). Clay content in the matrix of deformed rocks controls spacing and morphology of cleavage domains (Wanless, 1979; Marshak & Engelder, 1985).

The results of the present analysis indicate that sandstone beds at the western limb of the Sitagota syncline, where R_s values vary between 1.5 and 1.9, totally lack cleavage if bed thickness exceeds 50 mm. Beds with 30 mm thickness and associated with interbedded shale show most prominent cleavage fabric. However, similar 30 mm thick sandstone beds lack cleavage if associated with grit or conglomerate layers. Competency contrast in the form of shale beds alternating with thinner sandstone beds ($\sim$ 30 mm) seems to be critical to the development of cleavage within these rocks below R_s value of 1.9. While the shale interbeds became the preferred sites for development of cleavage seams, the latter eventually propagated across the sand–shale

interface and the sand layers ultimately became susceptible to cleavage development. However, control of lithology behind cleavage development becomes less prominent at $R_s > 1.9$, such as in the vicinity of the reverse fault at the western limb of the Pandripat syncline where, besides sandstone–shale intercalations, visible cleavage fabric is present even within coarse-grained layers of the Bortalao Formation as well as the Sitagota Volcanics. Hence, an R_s value of 1.9–2 is thought to be critical, above which the role of lithology diminishes, while below this critical value, lithological parameters such as bed thickness and competency contrasts become important for controlling cleavage development.

The critical grain size for cleavage development within the rocks of the Khairagarh Group is 0.036 mm (4.75 ϕ). Cleavage fails to develop above this grain size in the rocks, irrespective of varying strain intensity (R_s: 1.2–2.1). An impersistent cleavage (Type-I) develops between 0.030 mm and 0.036 mm (4.75–5 ϕ) grain size, while a persistent anastomosing cleavage (Type-II) develops below grain size of 0.030 mm ($> 5\ \phi$). Apparently, the fine-grained texture of the rock increased the total amount of grain boundary and thus interconnectivity within grains, and the rock became susceptible to deformation by rock–water interaction. The greater interconnectivity provided an important link between sites of dissolution on grain boundaries and the interstitial fluid of the rock, and the rock became susceptible to cleavage development. Thus, in contrast to bed thickness and competency contrast, influence of grain size on cleavage development persists even at R_s value of 2, so grain size plays a greater role in controlling cleavage development than other lithological parameters in low-strain ($R_s \approx 2$), low-grade belts.

7. Conclusions

(1) Analysis of the grain-scale deformation mechanisms reveals that deformation was accomplished by a combination of pressure solution, microfracturing and dislocation creep processes. Dislocation creep dominated initially and controlled early folding, while pressure solution coupled with microfracturing became important during a later stage of fold tightening and cleavage formation.

(2) If volume constancy during crustal-scale deformation is maintained, the association of pressure solution–microfracturing in combination with dislocation creep is suggested to be the characteristic grain-scale process at shallow crustal settings. This is particularly likely in low-grade–low-strain belts ($X/Z \approx 2$) where metamorphic grain growth and grain reorientation are less significant.

(3) The restricted nature of cleavage development within the rocks of the Khairagarh Group is dependent on layer thickness, grain size and competency contrast between alternating sandstone–shale beds. Layer thickness (~ 30 mm) and competency contrasts play a major role behind cleavage development at $R_s < 1.9$ and lose significance above this critical value. The control of finer grain size (~ 0.036 mm or 4.75 ϕ) persists above an R_s value of 1.9. However, further data on lithological parameters from such low grade–low strain belts is needed to assess fully the role of lithology behind cleavage development at shallow crustal depths.

Acknowledgements. We acknowledge the Department of Geology, Presidency College, Kolkata for providing us the infrastructural facilities during the present work. SC carried out this work as a part of her M.Sc. thesis in the Department of Geology, Presidency College, Kolkata. We thankfully acknowledge Prof. A. Maltman for a thorough and critical review of the earlier version of the manuscript.

References

ACHARYYA, S. K. & ROY, A. 2000. Tectonothermal history of the Central Indian tectonic zone and reactivation of major fault/shear zones. *Journal of the Geological Society of lndia* **55**, 239–56.

ALVAREZ, W., ENGELDER, T. & GEISER, P. A. 1978. Classification of solution cleavage in pelagic limestones. *Geology* **6**, 263–6.

BADERTSCHER, N. P. & BURKHARD, M. 2000. Brittle–ductile deformation in the Glarus Lochseiten (LK) calc-mylonite. *Terra Nova* **12**, 281–8.

BHOWMIK, S. K., PAL, T., ROY, A. & PANT, N. C. 1999. Evidence for PreGrenvillian High-Pressure Granulite Metamorphism from the Northern Margin of the Sausar Mobile Belt in Central India. *Journal of the Geological Society of lndia* **53**, 385–99.

BLENKINSOP, T. 2000. *Deformation Microstructures and Mechanisms in Minerals and Rocks*. Dordrecht, Boston, London: Kluwer Academic Publishers, 150 pp.

BRODIE, K. H. & RUTTER, E. H. 2000. Deformation mechanisms and rheology: why marble is weaker than quartzite. *Journal of the Geological Society, London* **157**, 1093–6.

COX, S. F. & ETHERIDGE, M. A. 1989. Coupled grain scale dilatancy and mass transfer during deformation at high fluid pressure: Examples from Mount Lyell, Tasmania. *Journal of Structural Geology* **11**, 147–62.

DE BOER, R. B. 1977. On the thermodynamics of pressure solution – interaction between chemical and mechanical forces. *Geochimica et Cosmochimica Acta* **41**, 249–56.

DE BRESSER, J. H. P., EVANS, B. & RENNER, J. 2002. Predicting the strength of calcite rocks under natural conditions. In *Deformation Mechanisms, Rheology and Tectonics: Current Status and Future Perspectives* (eds S. de Meer, M. R. Drury, J. H. P. de Bresser and G. M. Pennock), pp. 309–29. Geological Society of London, Special Publication no. 200.

DE PAOR, D. G. 1988. $R_{f-\phi}$ strain analysis using an orientation net. *Journal of Structural Geology* **10**, 323–33.

DESHPANDE, G. G., MOHABEY, N. K. & DESHPANDE, M. S. 1990. Petrography and tectonic setting of Dongargarh volcanics. *Geological Survey of India*, *Special Publication* **28**, 260–86.

DIETRICH, D. 1989. Fold axis parallel extension in an arcuate fold and thrust belt: the case of the Helvetic nappes. *Tectonophysics* **170**, 183–212.

DUNNET, D. W. 1969. A technique of finite strain analysis using elliptical particles. *Tectonophysics* **7**, 117–36.

ENGELDER, T. & MARSHAK, S. 1985. Disjunctive cleavage formed at shallow depths in sedimentary rocks. *Journal of Structural Geology* **7**, 327–43.

EVANS, M. A. & DUNNE, W. M. 1991. Strain factorization and partitioning in the North Mountain thrust sheet, central Appalachians, USA. *Journal of Structural Geology* **13**, 21–35.

FORD, M. 1990. The stratigraphy and structure of the Gallet Head Culmination Zone: an area of enhanced shortening related to basin geometry within the Irish Variscides. *Geological Journal* **25**, 145–59.

GANGOPADHYAY, P. K. & RAY, A. 1992. Petrochemical significance of basalt–rhyolite suite in Precambrians of Darekasa Amgaon Deori region of M. P. and Maharastra, Central India and suggestions of a possible greenstone sequence. *Indian Journal of Earth Science* **19**, 59–69.

GANGOPADHYAY, P. K. & RAY, A. 1997. Petrotectonic significance of rhyolite–granite suite of Dongargarh Supergroup of central India. *Indian Minerals* **57**, 123–36.

GHOSH, S. K. 1993. *Structural Geology: Fundamentals and Modern Developments*. Pergamon Press, 598 pp.

GRATIER, J. P., RENARD, F. & LABAUME, P. 1999. How pressure solution creep and fracturing processes interact in the upper crust to make it behave in both a brittle and viscous manner. *Journal of Structural Geology* **21**, 1189–97.

GRAY, D. R. & WILLMAN, C. E. 1991. Thrust related strain gradients and thrusting mechanisms in a chevron folded sequence, southeastern Australia. *Journal of Structural Geology* **13**, 691–710.

GROSHONG, R. H. JR. 1988. Low temperature deformation mechanisms and their interpretation. *Geological Society of America Bulletin* **100**, 1329–60.

HARRISON, M. J. & ONASCH, C. M. 2000. Quantitative assessment of low-temperature deformation mechanisms in a folded quartz arenite, Vallet and Ridge Province, West Virginia. *Tectonophysics* **317**, 73–91.

JAIN, S. C., YEDDEKAR, D. B. & NAIR, K. K. K. 1991. Central Indian shear zone: a major Precambrian crustal boundary. *Journal of the Geological Society of lndia* **37**, 521–30.

KNIPE, R. J. 1989. Deformation mechanisms – recognition from natural tectonites. *Journal of Structural Geology* **11**, 127–46.

KRISHNAMURTHY, P., SINHA, D. K., RAI, A. K., SETH, D. K. & SINGH, S. M. 1990. Magmatic rocks of the Dongargarh Supergroup, central India – their petrological evolution and implication on metallogeny. *Geological Survey of India, Special Publication* **28**, 303–19.

MARSHAK, S. & ENGELDER, T. 1985. Development of cleavage in limestones of a fold-thrust belt in eastern New York. *Journal of Structural Geology* **7**, 345–59.

MITRA, G. & ELLIOTT, D. 1980. Deformation of basement in the Blue Ridge and the development of South Mountain cleavage. In *The Caledonides of the U.S.A.* (ed. D. R. Wones), pp. 307–11. Virginia Polytechnic Institute and State University, Department of Geological Sciences, Memoir no. 2.

MUKHOPADHYAY, J., RAY, A., GHOSH, G., MEDDA, R. A. & BANDYOPADHYAY, P. P. 2001. Recognition, characterization and implications of high grade silicic ignimbrite facies from the Paleoproterozoic Bijli Rhyolites, Dongargarh Supergroup, Central India. *Gondwana Research* **4**, 519–27.

NEOGI, S., MIURA, H. & HARIYM, Y. 1996. Geochemistry of the Dongargarh volcanic rocks, central India: implications for Precambrian mantle. *Precambrian Research* **76**, 77–91.

POIRIER, J.-P. 1985. *Creep of crystals: high temperature deformation processes in metals, ceramics and minerals*. New York: Cambridge University Press, 260 pp.

RAMACHANDRA, H. M., MISHRA, V. P., ROY, A. & DUTTA, N. K. 1998. Evolution of the Bastar Craton – a critical review of gneiss-granitoids and supracrustal belts (Abstract). *M. S. Krishnan Centenary Commemorative National Seminar, Calcutta*, 144–50.

RAMACHANDRA, H. M. & ROY, A. 1998. Geology of intrusive granitoids with particular reference to Dongargarh granite and their impact on tectonic evolution of the Precambrian in Central India. *Indian Minerals* **52**, 15–33.

RAMACHANDRA, H. M., ROY, A., MISHRA, V. P., ROY, A. & DUTTA, N. K. 2001. A critical review of the tectonothermal evolution of the Bastar craton. *Geological Survey of India, Special Publication* **55**, 161–80.

RAMBERG, H. 1963. Strain distribution and geometry of folds. *Bulletin of the Geological Institute of the University of Uppsala* **42**, 1–20.

RAMSAY, J. G. 1967. *Folding and fracturing of rocks. New York*: McGraw-Hill, 568 pp.

RAMSAY, J. G. & HUBER, M. I. 1983. *Techniques of Modern Structural Geology: 1. Strain Analysis. London:* Academic Press, 307 pp.

RATTEY, P. R. & SANDERSON, D. J. 1982. Patterns of folding within nappes and thrust sheets: examples from the Variscan of southwest England. *Tectonophysics* **88**, 247–67.

ROO, J. A. DE & WILLIAMS, P. F. 1990. Dynamic recrystallization and solution transfer in mylonitic rocks of Tetagouche Group, Northern New Brunswick, Canada. *Geological Society of America Bulletin* **102**, 1544–54.

ROY, A., RAMACHANDRA, H. M. & BANDYOPADHYAY, B. K. 2000. Supracrustal belts and their significance in the crustal evolution of Central India. *Geological Survey of India, Special Publication* **55**, 361–80.

SARKAR, S. N. 1957–58. Stratigraphy tectonics of the Dongargarh System, a new system in the Precambrians of Bhandara-Durg-Balaghat area, Bombay and Madhya Pradesh. *Journal of Science and Engineering Research, I.I.T. Kharagpur, India* **1**, 145–60.

SARKAR, S. N., GERLING, E. K., POLKANOV, A. A. & CHUKROV, F. V. 1967. Precambrian geochronology of Nagpur-Bhandara-Durg, India. *Geological Magazine* **104** 525–49.

SARKAR, S. N., GOPALAN, K. & TRIVEDI, J. R. 1981. New data on the geochronology of the precambrians of Bhandara-Durg, Central India. *Indian Journal of Earth Science* **8**, 131–51.

SARKAR, S. N., SARKAR, S. S. & RAY, S. L. 1994. Geochemistry and genesis of the Dongargarh Supergroup Precambrian rocks in Bhandara-Durg region, Central India. *Indian Journal of Earth Science* **21**, 114–26.

TULLIS, J. & YUND, R. 1985. Dynamic recrystallization of feldspar: A mechanism for ductile shear zone formation. *Geology* **13**, 238–41.

WANLESS, H. 1979. Limestone response to stress: pressure solution and dolomitization. *Journal of Sedimentary Petrology* **49**, 437–62.

WILLIAMS, P. F. 1972. Development of metamorphic layering and cleavage in low grade rocks at Bermagui, Australia. *American Journal of Science* **272**, 1–47.

WU, S. & GROSHONG, R. H. JR. 1991. Low temperature deformation of sandstone, southern Appalachian fold-thrust belt. *Geological Society of America Bulletin* **103**, 861–75.

YASSAGHI, A., JAMES, P. R. & FLOTTMANN, T. 2000. Geometric and kinematic evolution of asymmetric ductile shear zones in thrust sheets, southern Adelaide fold-thrust belt, South Australia. *Journal of Structural Geology* **22**, 889–912.

YEDDEKAR, D. B., JAIN, S. C., NAIR, K. K. K. & DUTTA, K. K. 1990. The central Indian Collision suture. *Geological Survey of India, Special Publication* **28**, 1–43.